

Nanoparticle Surfactants as a Route to Bicontinuous Block Copolymer Morphologies

Bumjoon J. Kim,^{†,‡} Glenn H. Fredrickson,^{†,‡,§} Craig J. Hawker,^{†,§,||} and Edward J. Kramer^{*,†,‡,§}

Materials Research Laboratory, Department of Chemical Engineering, Department of Materials, and Department of Chemistry and Biochemistry, University of California, Santa Barbara, California 93016

Received February 21, 2007. In Final Form: April 6, 2007

The surface chemistry of nanoparticles can be modified so that these particles behave like surfactants and localize at interfaces between two fluids. We demonstrate that small volume fractions ϕ_p of such surfactant nanoparticles added to lamellar diblock copolymers lead initially to a decrease in lamellar thickness with ϕ_p , a consequence of decreasing interfacial tension, up to a critical value of ϕ_p , beyond which the block copolymer adopts a bicontinuous morphology. These bicontinuous morphologies have stable domain spacings below 100 nm that further decrease with increasing ϕ_p and offer new routes to nanoscopically engineered polymer films with potential photovoltaic, fuel cell, and battery applications.

Introduction

Bicontinuous polymeric structures have attracted considerable interest for use as photovoltaic films,^{1,2} as membranes for the transport of ionic species in fuel cells/batteries and small molecules in barrier films and so forth.^{3–5} Self-assembled polymeric materials are particularly appealing in these applications where co-continuous polymer phases, for example, hydrophobic and hydrophilic, combine ease of processing, mechanical integrity, and a high moisture absorption rate and capacity. Polymeric systems also allow the removal of one phase, creating a porous, high-surface-area structure that can be used in applications ranging from separations to thermal management.⁶ Therefore, it is important to seek possible routes^{7–11} to achieve stable bicontinuous structures with domain spacings well below 100 nm, which would be ideal for optimizing mechanical and transport properties.

In examining robust strategies for creating and stabilizing these novel morphologies, traditional approaches based on melt mixing or casting binary polymer blends from a common solvent typically lead to gross macrophase separation and nonviable materials. The quenching of a spinodal decomposition process followed by

trapping of the nonequilibrium structure can produce desirable bicontinuous microstructures.¹² Subsequent thermal processing, however, can destroy the bicontinuous morphology. Similarly rapid solvent casting can lead to bicontinuous morphologies that are far from equilibrium. In contrast, microphase-separated block copolymers can themselves possess equilibrium bicontinuous morphologies, the most common of which, for AB diblock copolymers, is the periodic cubic phase termed the double gyroid (*Ia3d* space group).^{3,4} The addition of an A-*b*-B diblock copolymer to a binary A-B homopolymer blend can also lead to formation of a thermodynamically stable bicontinuous microemulsion similar to oil/water microemulsions stabilized by amphiphilic surfactants for certain compositions and molecular weights.^{7,8} The addition of an A-B-A triblock copolymer to the low-molecular-weight A homopolymer has also been observed to produce a bicontinuous L₃ symmetric sponge phase.¹¹ Recently, as a result of careful design, polymeric bicontinuous microemulsions have been created by in situ reactive compounding to form a complex mixture of homopolymers and random graft copolymers.¹⁰

Here we demonstrate that nanoparticles can act as surfactants for block copolymers, leading to stable bicontinuous morphologies with characteristic dimensions of less than 100 nm. At low nanoparticle volume fractions, nanoparticles with controlled surface chemistry will assemble either in the A/B domains or at the A-B interface of an A-*b*-B copolymer and can enhance optical properties,¹³ create efficient catalysts,¹⁴ or produce chemical/biological sensors.¹⁵ Larger surfactant colloids in two-phase fluid systems can form Pickering emulsions by decreasing the interfacial tension and stabilizing the liquid film between droplets, thus preventing coalescence.¹⁶ Recent simulations¹⁷ and experiments¹⁸ suggest that nanoparticle surfactants may stabilize bicontinuous emulsions of small-molecule liquids as well as

* To whom correspondence should be addressed. E-mail: edkramer@mrl.ucsb.edu.

[†] Materials Research Laboratory.

[‡] Department of Chemical Engineering.

[§] Department of Materials.

^{||} Department of Chemistry and Biochemistry.

(1) Ma, W. L.; Yang, C. Y.; Gong, X.; Lee, K.; Heeger, A. J. *Adv. Funct. Mater.* **2005**, *15*, 1617–1622.

(2) Sivula, K.; Luscombe, C. K.; Thompson, B. C.; Frechet, J. M. J. *J. Am. Chem. Soc.* **2006**, *128*, 13988–13989.

(3) Chan, V. Z. H.; Hoffman, J.; Lee, V. Y.; Iatrou, H.; Avgeropoulos, A.; Hadjichristidis, N.; Miller, R. D.; Thomas, E. L. *Science* **1999**, *286*, 1716–1719.

(4) Hashimoto, T.; Tsutsumi, K.; Funaki, Y. *Langmuir* **1997**, *13*, 6869–6872.

(5) Ulbricht, M. *Polymer* **2006**, *47*, 2217–2262.

(6) Hillmyer, M. A. *Adv. Polym. Sci.* **2005**, *190*, 137–181.

(7) Bates, F. S.; Maurer, W. W.; Lipic, P. M.; Hillmyer, M. A.; Almdal, K.; Mortensen, K.; Fredrickson, G. H.; Lodge, T. P. *Phys. Rev. Lett.* **1997**, *79*, 849–852.

(8) Hillmyer, M. A.; Maurer, W. W.; Lodge, T. P.; Bates, F. S.; Almdal, K. *J. Phys. Chem. B* **1999**, *103*, 4814–4824.

(9) Pei, Q. B.; Yu, G.; Zhang, C.; Yang, Y.; Heeger, A. J. *Science* **1995**, *269*, 1086–1088.

(10) Pernot, H.; Baumert, M.; Court, F.; Leibler, L. *Nat. Mater.* **2002**, *1*, 54–58.

(11) Falus, P.; Xiang, H.; Borthwick, M. A.; Russell, T. P.; Mochrie, S. G. *J. Phys. Rev. Lett.* **2004**, *93*, Art. 145701.

(12) Aubert, J. H.; Clough, R. L. *Polymer* **1985**, *26*, 2047–2054.

(13) Bockstaller, M. R.; Thomas, E. L. *J. Phys. Chem. B* **2003**, *107*, 10017–10024.

(14) Jaramillo, T. F.; Baeck, S. H.; Cuenya, B. R.; McFarland, E. W. *J. Am. Chem. Soc.* **2003**, *125*, 7148–7149.

(15) Bruns, N.; Tiller, J. C. *Nano Lett.* **2005**, *5*, 45–48.

(16) Binks, B. P. *Curr. Opin. Colloid Interface Sci.* **2002**, *7*, 21–41.

(17) Stratford, K.; Adhikari, R.; Pagonabarraga, I.; Desplat, J. C.; Cates, M. E. *Science* **2005**, *309*, 2198–2201.

(18) Chung, H.; Ohno, K.; Fukuda, T.; Composto, R. J. *Nano Lett.* **2005**, *5*, 1878–1882.

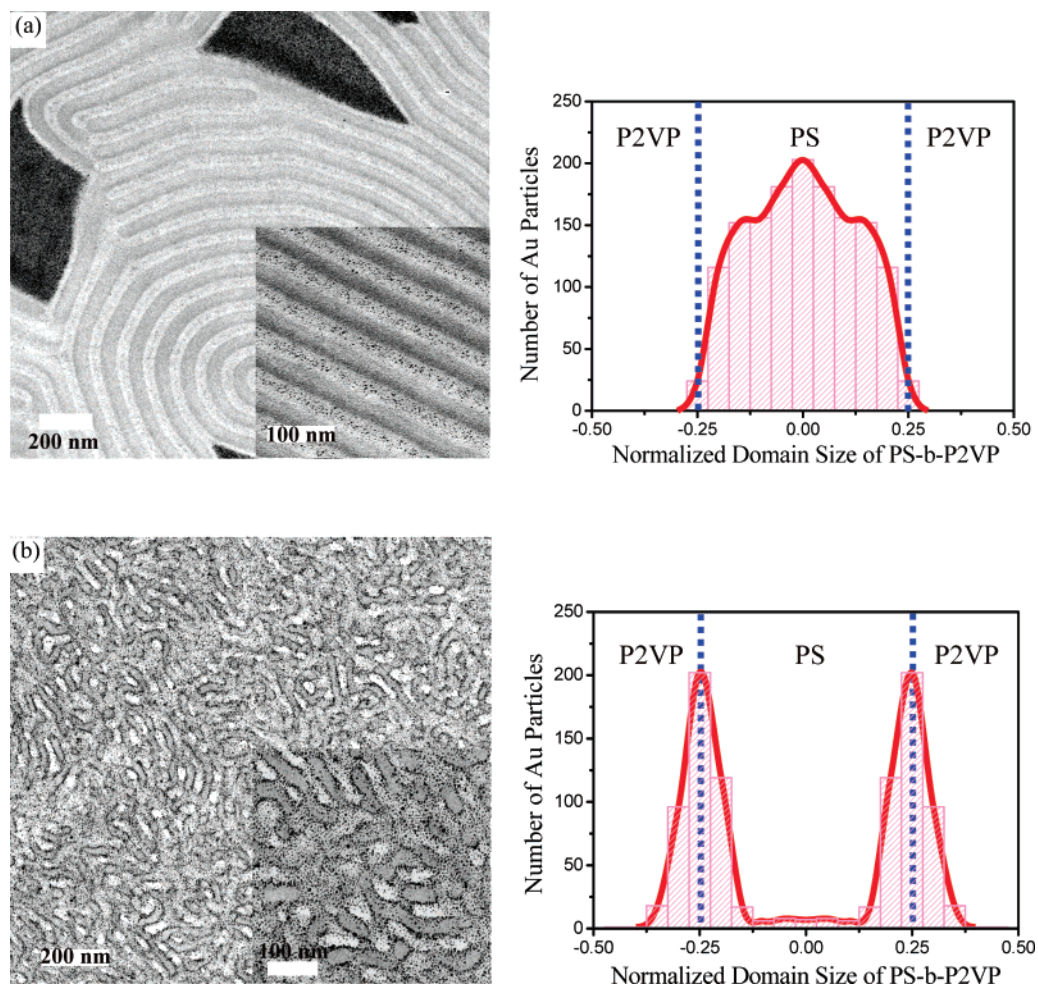


Figure 1. Effect of nanoparticle location on the morphology of a symmetric PS-*b*-P2VP block copolymers ($M_n = 196$ kg/mol). (a) PS-*b*-P2VP mixed with 0.20 volume fraction (ϕ_p) PS-Au 2.38 gold nanoparticles ($\Sigma = 2.38$ chains/nm²) that segregate to the PS domains. Lamellar domains with a low volume fraction of gold nanoparticles are seen together with macrophase-separated gold-nanoparticle-rich regions (very dark). (b) PS-*b*-P2VP mixed with $\phi_p = 0.14$ PS-Au 0.92 gold nanoparticles ($\Sigma = 0.92$ chains/nm²) that segregate to the PS/P2VP domain interface. A bicontinuous PS-*b*-P2VP morphology on the sub-100-nm length scale is observed. The histograms show the nanoparticle positions of PS-Au 2.38 (top) and PS-Au 0.92 (bottom) within PS-*b*-P2VP domains for $\phi_p \approx 0.035$. Because the lamellar thickness of the PS domain is normalized to 0.5, the center of the PS domain is at 0, and the interfaces of the PS domain are at -0.25 and $+0.25$.

bicontinuous morphologies in two-phase blends of A and B homopolymers. These studies assume such emulsions to be metastable, with an initial bicontinuous microstructure resulting from spinodal decomposition of the liquid or the polymer mixture being arrested by the “jamming” of nanoparticles that are strongly adsorbed to the liquid/liquid or polymer/polymer interfaces.

In this article, we report an entirely different approach to achieving a fine scale bicontinuous polymeric morphology that does not rely on jamming of the nanoparticles. We show that increasing volume fractions of Au nanoparticle surfactants, designed to segregate to the interfaces of the lamellar diblock copolymer PS-*b*-P2VP (a single component), first cause a decrease in the lamellar period and then beyond a critical volume fraction, which decreases as the molecular weight of the block copolymer increases, give rise to stable bicontinuous block polymer microstructures with characteristic dimensions well below 100 nm. Bicontinuous microstructures with such small dimensions are ideally suited for many of the emerging applications discussed above. The initial shrinkage of the lamellar spacing is directly caused by the decrease in block copolymer interfacial tension that results from nanoparticle segregation, and the magnitude of the shrinkage is qualitatively predicted by the recent strong segregation theory of Pryamitsyn and Ganesan, a theory that also predicts that the lamellar-to-bicontinuous transition is caused

by a decrease in the bending modulus of the lamellae as nanoparticles are added to the interface.

Experimental Procedures

Synthesis of Polymers and Polymer-Coated Gold Nanoparticles. Thiol-terminated PS (PS-SH) with a molecular weight (M_n) of 2.5 kg/mol and a polydispersity index (PDI) of 1.1 was synthesized by living anionic polymerization and characterized as described elsewhere.^{19,20} Thiol-terminated random copolymers of styrene and 2-vinylpyridine (PS-*r*-P2VP-SH) were synthesized by reversible addition fragmentation transfer (RAFT) procedures,²¹ a dithioester RAFT agent, and AIBN at 70 °C. The polymer end group was converted to a thiol group by reaction with hexyl amine. The conversion during RAFT polymerization was kept as low as 0.12 to prevent the composition drift caused by the difference in the reactivity ratio of the styrene and 2-VP monomers. The M_n and PDI of PS-*r*-P2VP were 3.5 kg/mol and 1.1, respectively, with the mole fraction of styrene in PS-*r*-P2VP found to be 0.52 by ¹H NMR. The synthesis of PS-coated Au nanoparticles was accomplished using a

(19) Kim, B. J.; Bang, J.; Hawker, C. J.; Kramer, E. J. *Macromolecules* **2006**, *39*, 4108–4114.

(20) Kim, B. J.; Given-Beck, S.; Bang, J.; Hawker, C. J.; Kramer, E. J. *Macromolecules* **2007**, *40*, 1796–1798.

(21) Drockenmüller, E.; Li, L. Y. T.; Ryu, D. Y.; Harth, E.; Russell, T. P.; Kim, H. C.; Hawker, C. J. *Journal of Polymer Science Part A-Polymer Chemistry* **2005**, *43*, 1028–1037.

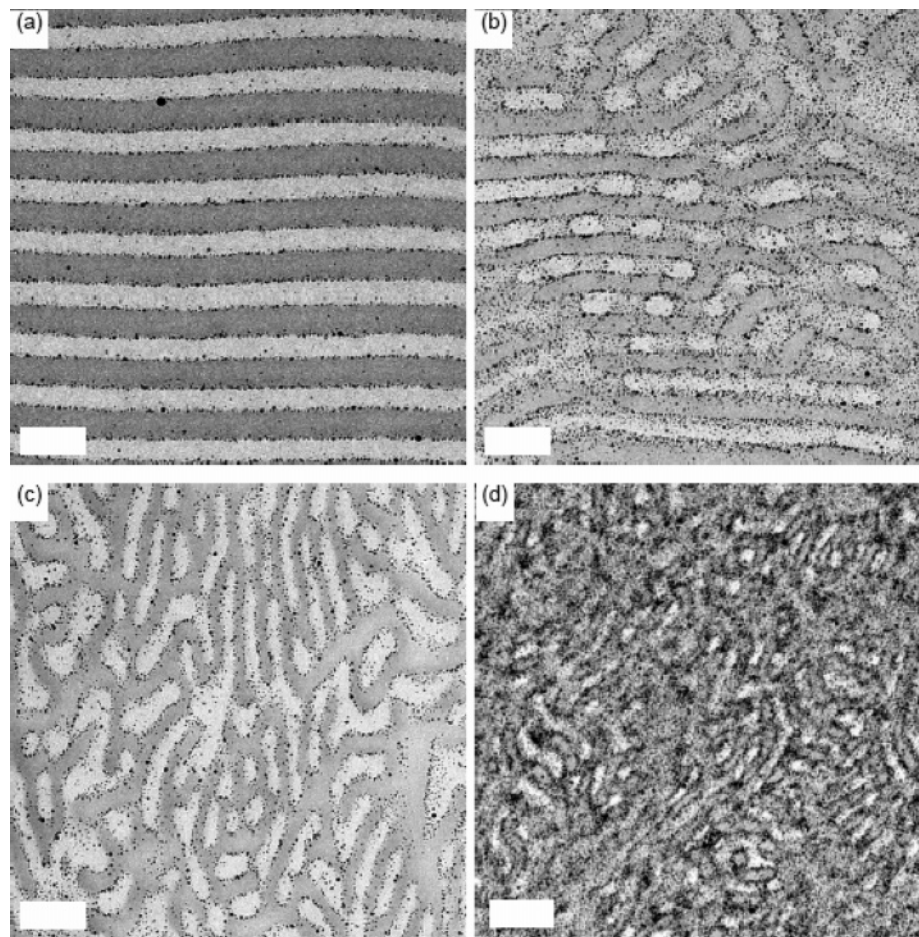


Figure 2. Cross-sectional TEM images of PS-*b*-P2VP block copolymer ($M_n = 196$ kg/mol) containing PS-Au 0.92 nanoparticles at various nanoparticle volume fractions (ϕ_p): (a) 0.04, (b) 0.07, (c) 0.09, and (d) 0.28. The scale bar is 100 nm. A well-ordered lamellar microstructure is seen with the gold nanoparticles (dark dots) segregated at the interfaces between the PS and P2VP domains in part a. As the volume fraction of PS-Au 0.92 nanoparticles is increased, the microstructure of the PS-*b*-P2VP diblock copolymer changes dramatically. Part c shows that when 9% by volume of the PS-SH-coated nanoparticles is added, the microstructure of the PS and P2VP domains becomes bicontinuous.

two-phase system²² consisting of toluene and water with two different initial mole feed ratios of PS ligands to gold atoms of 0.33 and 0.0625. As a result, two kinds of PS-coated Au nanoparticles were obtained with different areal densities (Σ) of PS chains on Au nanoparticles. ($\Sigma = 2.38$ and 0.92 chains/nm² (PS-Au 2.38 and PS-Au 0.92)). The synthesis of PS-*r*-P2VP-SH-coated Au nanoparticles was performed using a one-phase method with THF as described elsewhere.²³

Preparation of the Block Copolymer/Nanoparticle Composite Film. Three different symmetric poly(styrene-*b*-2-vinyl-pyridine) (PS-*b*-P2VP) diblock copolymers with various molecular weights (M_n) of ~ 114 , 190, and 380 kg/mol (Polymer Source, Inc.) were used as the block copolymer templates. For each block copolymer, a 1 to 2 wt % block copolymer solution in dichloromethane, which is a neutral solvent for the PS and P2VP blocks,²⁴ was mixed with gold nanoparticles to produce various volume fractions ranging from 0.01 to 0.53 in the final block copolymer/nanoparticle film. A nanoparticle/block copolymer composite film was prepared by solvent casting this mixture of gold nanoparticles and PS-*b*-P2VP block copolymer onto an epoxy substrate and then annealing under a saturated solvent atmosphere at 25 °C for at least a day. All solvent in the sample was allowed to evaporate very slowly over an additional

day. Samples were subsequently dried in air overnight and further under vacuum for 4 h to make sure that no solvent was left in the sample.

Characterization. The size of the polymer-coated gold nanoparticles and the location of the Au nanoparticles in the PS-*b*-P2VP block copolymer were determined by transmission electron microscopy (TEM) using a FEI Tecnai G2 microscope operated at 200 kV. To characterize the size of the gold nanoparticles, they were dissolved at a very low concentration in dichloromethane or THF. A TEM grid coated with a 20-to-30 nm thick carbon film was dipped into the solution for 1 s, dried in air, and then examined by TEM. The gold-core diameter distribution obtained from TEM image analysis was used to calculate the average surface area per gold nanoparticle. Weight fractions of gold and polymer ligands were measured by thermal gravimetric analysis. These numbers were confirmed by elemental analysis. The areal densities of polymer chains (Σ) on Au nanoparticles were estimated as described elsewhere.^{19,20} Samples of gold nanoparticle-block copolymer composites were prepared for cross-sectional TEM by microtoming epoxy-supported thick films into 25–40 nm slices that were then stained by exposing them to iodine vapor that selectively stains the P2VP domains. The thicknesses of the lamellar block copolymer morphology with and without nanoparticles as well as domain sizes of the bicontinuous morphology were determined by image analysis of multiple TEM micrographs for each sample. Tilt sequence images were taken at intervals of 1° tilt from -50 to $+50$ ° and 2.5° tilt from both -65 to -50 ° and $+50$ to $+65$ °, respectively, of samples with suspected bicontinuous morphology to be sure that the morphology

(22) Brust, M.; Walker, M.; Bethell, D.; Schiffrin, D. J.; Whyman, R. *Journal of the Chemical Society-Chemical Communications* **1994**, (7), 801–802.

(23) Yee, C. K.; Jordan, R.; Ulman, A.; White, H.; King, A.; Rafailovich, M.; Sokolov, J. *Langmuir* **1999**, *15*, 3486–3491.

(24) Kim, B. J.; Chiu, J. J.; Yi, G. R.; Pine, D. J.; Kramer, E. J. *Adv. Mater.* **2005**, *17*, 2618–2622.

was in fact bicontinuous. (See Supporting Information for a video of a typical tilt sequence.)

Results

The key to forming surfactant nanoparticles is the modification of the nanoparticle surface to create a “neutral” surface relative to the polystyrene (PS) and poly(2-vinylpyridine) (P2VP) blocks of the PS-P2VP block copolymer, resulting in strong nanoparticle localization at PS-P2VP interfaces. Such Au nanoparticles are tailored by coating them with short polymer chains using a “grafting-to” method with thiol linkages. Because P2VP segments are preferentially attracted to the bare gold nanoparticle surface over PS segments, attaching short PS chains to the nanoparticles at a low areal density exposes bare Au to the surrounding medium and leads to favorable interactions of the adsorbed PS chains with the PS block and favorable interaction of the bare Au with the P2VP block.²⁵ As a result, the strong adsorption of such partially PS-coated nanoparticles to the interface occurs,¹⁹ and if diffusion of the thiol-bonded PS chains on the gold nanoparticle surface is possible,^{26,27} then even stronger adsorption to PS/P2VP interfaces may well occur by redistribution of PS-thiols on the nanoparticles, creating “Janus” nanoparticles at the interface.

Exploiting this strategy, 1.42 (± 0.40) nm radius Au nanoparticles with grafted thiol-terminated PS (PS-SH) chains ($M_n \approx 2.5$ kg/mol) at an areal density (Σ) of 0.92 chains/nm² (PS-Au 0.92) were synthesized. Such nanoparticles are strongly localized at PS-P2VP interfaces. A second batch of nanoparticles with a larger areal density of PS-SH, 2.38 chains/nm² (PS-Au 2.38), were also prepared and were found to localize inside PS domains rather than at PS-P2VP interfaces. The two samples of gold nanoparticles were independently mixed into a symmetric PS-*b*-P2VP ($M_n = 196$ kg/mol) copolymer by a solvent casting procedure, and the bulk morphologies were examined by cross-section transmission electron microscopy (TEM).

Figure 1a shows the result of mixing the PS-Au 2.38 gold nanoparticles with PS-P2VP at a nanoparticle volume fraction (ϕ_p) of 0.20. The TEM image and corresponding histogram show that the lamellar mesophase of the neat block copolymer is preserved and that the nanoparticles are localized in the PS domains of the block copolymer. However, large regions of aggregated nanoparticles are also present at this nanoparticle loading, indicating coexistence between a macrophase that is highly enriched in nanoparticles and a lamellar mesophase with a much lower nanoparticle concentration.

In contrast, Figure 1b shows that the interfacially active nanoparticles, PS-Au 0.92, cause a dramatic change in the morphology of the composite. At a nanoparticle loading of $\phi_p \approx 0.14$, there is no sign of macrophase separation, and the nanoparticles are seen to be strongly localized at the PS-P2VP interfaces. Moreover, the nanoparticles have caused a uniform disruption of the block copolymer lamellar phase, instead creating a bicontinuous morphology of interpenetrating PS and P2VP domains that resembles a microemulsion. This bicontinuous structure is remarkable both in its uniformity and in the fine scale, ~ 25 nm, of the domains. The histogram in Figure 1b, obtained from a corresponding TEM image at a much lower nanoparticle loading ($\phi_p \approx 0.035$), shows that virtually all of the nanoparticles are segregated to the PS/P2VP interfaces.

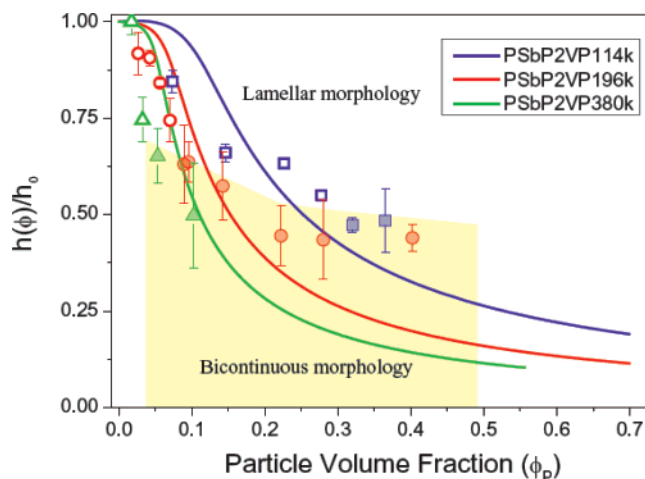


Figure 3. Phase diagram of PS-*b*-P2VP morphologies plotted as normalized lamellar domain size vs volume fraction of gold nanoparticles strongly bound to the interface. PS-Au 0.92 nanoparticles are dispersed into three different PS-*b*-P2VP diblock copolymers with M_n values of 114 kg/mol (blue squares), 196 kg/mol (red circles), and 380 kg/mol (green triangles). As the volume fraction of nanoparticles is increased, the nanoparticle/PS-*b*-P2VP morphology changes from lamellar (open symbols) to bicontinuous (filled symbols). The lines (blue, 114 kg/mol; red, 196 kg/mol; green, 380 kg/mol) correspond to the predictions of strong segregation theory.²⁹ Macrophase separation is not observed at $\phi_p = 0.52$ for PS-*b*-P2VP ($M_n = 196$ kg/mol) and $\phi_p = 0.43$ for PS-*b*-P2VP ($M_n = 114$ kg/mol).

It is particularly remarkable that bicontinuous microstructures are found over an extremely wide range of experimental conditions. For the system shown in Figure 1b, the microstructure remains bicontinuous as ϕ_p varies from 0.07 to 0.52.

Representative TEM images of PS-*b*-P2VP domains with various ϕ_p values are shown in Figure 2 and demonstrate that a dramatic change in the morphology of PS-*b*-P2VP from a well-aligned lamellar phase to a bicontinuous structure occurs as ϕ_p is increased from 0.04 to 0.09; even at $\phi_p \approx 0.40$, the bicontinuous structure remains surprisingly uniform. Note that the scale of the bicontinuous morphology decreases as ϕ_p increases. As described below, a decrease in the domain size of the block copolymer with ϕ_p , even within the lamellar morphology, reflects a decrease in interfacial tension upon surfactant nanoparticle addition and a concomitant increase in the block copolymer interfacial area.

To further illustrate the generality of this novel method for producing bicontinuous morphologies, a series of symmetric PS-P2VP diblock copolymers with M_n ranging from 114 to 380 kg/mol were blended with PS-Au 0.92 nanoparticles over a range of ϕ_p values.

Figure 3 shows a 2D phase diagram for the mixture plotted as h/h_0 versus ϕ_p , where h_0 is the lamellar thickness (half of the lamellar period) without added nanoparticles and h is the corresponding value at nanoparticle volume fraction ϕ_p .

For all three PS-*b*-P2VP polymers, the lamellar thickness decreases dramatically as ϕ_p is initially increased from zero, followed by an abrupt transition in morphology from lamellar to bicontinuous at a value of ϕ_p that decreases with an increase in M_n . The decrease in domain thickness in both the lamellar and bicontinuous morphologies creates additional interfacial area to accommodate more gold nanoparticles along the block copolymer interface. This increase in interfacial area cannot be due to nanoparticle jamming because even if one assumes that all nanoparticles are localized at the interface, nanoparticle area fractions a_f never exceed 0.6 before the transition to the bicontinuous morphology occurs and large increases in interfacial

(25) Kunz, M. S.; Shull, K. R.; Kellock, A. J. *J. Colloid Interface Sci.* **1993**, *156*, 240–249.

(26) Jackson, A. M.; Myerson, J. W.; Stellacci, F. N. *Nat. Mater.* **2004**, *3*, 330–336.

(27) Shan, J.; Nuopponen, M.; Jiang, H.; Viitala, T.; Kauppinen, E.; Kontturi, K.; Tenhu, H. *Macromolecules* **2005**, *38*, 2918–2926.

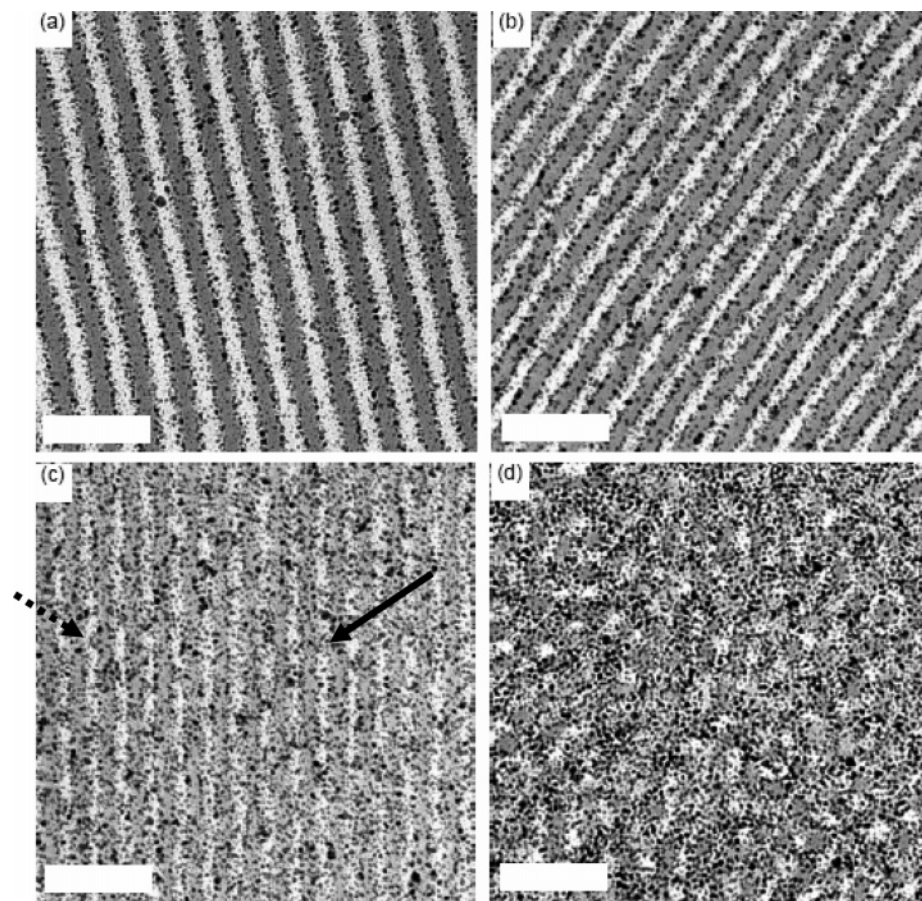


Figure 4. Cross-sectional TEM images of a PS-*b*-P2VP block copolymer ($M_n = 114$ kg/mol) containing PS-Au 0.92 nanoparticles at various nanoparticle volume fractions (ϕ_p): (a) 0.23, (b) 0.28, (c) 0.32, and (d) 0.42. The scale bar is 100 nm. These results provide strong evidence that the bicontinuous structure is not kinetically trapped but is nearly in equilibrium. At $\phi_p = 0.23$ and 0.28, well-ordered lamellar morphology accommodating densely packed gold nanoparticles at the interface is observed with almost no defects within a large area of a few tens of square micrometers. With a slight increase in ϕ_p from 0.28 to 0.32, the interfaces of the lamellar structure develop some perturbations (e.g., at the dashed arrow), and the lamellar domains start to develop interconnections (an example is shown at the solid arrow). Finally, at $\phi_p = 0.37$ (not shown) and 0.42 the bicontinuous morphology is fully developed. The transition thus occurs dramatically over a narrow ϕ_p range from a well-aligned lamellar structure without defects at $\phi_p = 0.23$ and 0.28, just below $\phi_{p,BC}$. These observations, along with the slow solvent annealing procedure employed, suggest that the bicontinuous structure observed is at or near equilibrium.

area and decreases in lamellar thickness are observed at an a_f value as low as 0.2. Of particular interest is that the critical nanoparticle volume fraction necessary to induce the bicontinuous phase ($\phi_{p,BC}$) increases dramatically from 0.04 ($a_f \approx 0.2$) to 0.3 ($a_f \approx 0.55$) as the PS-*b*-P2VP M_n is decreased from 380 to 114 kg/mol. Cross-sectional TEM images of the lowest molecular weight PS-*b*-P2VP block copolymer ($M_n = 114$ kg/mol) blended with PS-Au 0.92 in Figure 4 clearly show that the morphology changes from well-ordered lamellar to fully bicontinuous as ϕ_p increases from 0.28 to 0.32, providing evidence that the bicontinuous structure is in equilibrium rather than kinetically trapped.

Discussion

“Strong segregation” models²⁸ of block copolymer morphology can help explain the decrease in lamellar thickness and increase in interfacial area on adding surfactant nanoparticles. The free energy per chain of a lamellar AB diblock copolymer includes two additive terms: an entropy loss caused by stretching of the blocks from the interface that increases as h^2 and a term representing the interfacial area per chain times the AB interfacial energy γ_{AB} , which scales as h^{-1} . This model leads to an

equilibrium value for $h \approx (\gamma_{AB} a^2 N^2 / (3\rho_0 k_B T))^{1/3}$, where a is the polymer statistical segment length, N is the polymerization index, ρ_0 is the segment density, k_B is Boltzmann’s constant, and T is temperature. A segregation of surfactant nanoparticles to the interface leads to a decrease in interfacial tension and a corresponding decrease in h , allowing the stretching of the blocks to be decreased. Conversely, the decrease in h observed as nanoparticles adsorb to the interface is evidence of their action as surfactants. Significantly, a strong segregation theory treatment of surfactant nanoparticles in block copolymers that qualitatively predicts many of the features that we see in our experiments has recently been developed.²⁹ This treatment by Pryamitsyn and Ganesan predicts that the decrease in h is dependent only on R/h_0 , where R is the radius of the nanoparticles. For our nanoparticles, the predictions shown by the lines in Figure 3 are in qualitative agreement with our experiments. Most importantly, as h/h_0 decreases, the bending modulus of the lamellae decreases, producing an instability that ultimately results in the formation of bicontinuous morphology. It is notable that their calculation²⁹ suggests that the lamellar-to-bicontinuous transition is driven by a vanishing of the bending modulus for mean curvature, K , rather than variations in the saddle splay modulus, \bar{K} , as is invoked in

(28) Semenov, A. N. *Zhurnal Eksperimentalnoi I Teoreticheskoi Fiziki* **1985**, *88*, 1242–1256.

(29) Pryamitsyn, V.; Ganesan, V. *Macromolecules* **2006**, *39*, 8499–8510.

the L_{α} -to L_3 transition of lyotropic surfactants.³⁰ They predict a critical nanoparticle volume fraction of $\phi_{P,BC} \approx 0.8(R/h_0)^{1/2} - 0.1R/h_0$. This approximate relation predicts $\phi_{P,BC} \approx 0.24$ for the 114 kg/mol block copolymer, decreasing to a value of 0.16 for the 380 kg/mol copolymer. Their prediction is in reasonable agreement with our value for the lower-molecular-weight block copolymer and qualitatively captures the decrease in $\phi_{P,C}$ seen in Figure 3 as M_n increases, but the predicted decrease is much smaller than that seen in our experiments. The discrepancy may be caused by slight asymmetries in the block copolymer/nanoparticle system (the theory assumes that the nanoparticles are strongly adsorbed so that they are situated symmetrically across the interface) or by various approximations of the strong segregation calculation. More accurate hybrid particle field³¹ or DFT-S-CFT simulations³² of these polymer nanocomposites should yield an improved description of the lamellar-to-bicontinuous transition.

We have demonstrated the formation of a bicontinuous phase in PS-*b*-P2VP induced by Au nanoparticles that are only partially covered by PS ligands. Theoretically, however, any nanoparticle with an approximately “neutral” surface relative to the A and B polymers will bind to the interface as long as the interfacial tension of the A/B interface is large enough. If the interfacial binding is sufficiently strong, then it should again be possible to avoid macroscopic phase separation of nanoparticles and obtain bicontinuous morphology. To prove this concept, we prepared Au nanoparticles coated with a thiol-terminated random copolymer of styrene and 2-vinylpyridine (PS-*r*-P2VP-SH). The PS-*r*-P2VP-SH ligands, which have a M_n of 3.5 kg/mol and a narrow PDI of 1.1, were synthesized by controlled radical polymerization.²¹ The PS molar fraction of the random copolymer was 0.52 to approximate a neutral coating on the nanoparticle surface, and the areal density was $\Sigma \approx 1.61$ chains/nm². The resulting gold nanoparticles were mixed with PS-*b*-P2VP ($M_n = 196$ kg/mol) at nanoparticle volume fractions (ϕ_P) of 0.05 and 0.2, and the sample was solvent annealed as before. Cross-sectional TEM analysis of the composition at $\phi_P = 0.05$ shows well-ordered lamellar domains with gold nanoparticles localized at the interfaces, but at $\phi_P = 0.20$, macrophase-separated domains of nanoparticles are observed. However, when the random-

copolymer-coated nanoparticles were blended at a composition of $\phi_P \approx 0.15$ with the higher-molecular-weight block copolymer PS-*b*-P2VP ($M_n = 380$ kg/mol), TEM analysis (Supporting Information, video 1) reveals bicontinuous morphology with no macrophase separation. By analogy with the findings of Figure 3 based on the PS-coated Au nanoparticles, the threshold for forming the bicontinuous structure, $\phi_{P,BC}$, and the tendency toward macrophase separation are reduced by increasing the molecular weight of the host matrix. We think that the reason that the random copolymer “neutral” surfactant particles are less effective at inducing bicontinuous morphology than the PS-Au 0.92 particles may be due to a Janus structure of the PS-Au 0.92.

Conclusions

In summary, a general, robust method for the fabrication of stable bicontinuous polymeric phases with domains below 100 nm has been developed. The method involves blending symmetric AB diblock copolymers with surfactant nanoparticles whose surfaces are treated to promote strong binding to the A/B interfaces while avoiding macrophase separation. The method has implications for a variety of applications that require a continuous phase for the transport of molecular species, ions, or electrons and a second phase for mechanical support or the conduction of a separate species. Furthermore, the materials that can be fabricated by this method are potentially enhanced by the electrical, optical, magnetic, and/or catalytic properties of the inorganic nanoparticles incorporated into the bicontinuous structure.

Acknowledgment. This work was supported by the MRSEC Program of the National Science Foundation under award DMR05-20418. We acknowledge Venkat Ganesan and Frank Bates for stimulating discussions and the former for sending us his preprint. We acknowledge the contribution from Joona Bang and Se Gyu Jang to the RAFT polymerization of the random copolymer ligands and the image analysis of the nanoparticle size distribution.

Supporting Information Available: Tilt sequence of TEM micrographs of a 380 kg/mol PS-*b*-P2VP block copolymer with a volume fraction of 0.15 for random-copolymer-coated gold nanoparticles. The images were taken at intervals of 1° tilt from -50 to +50° and 2.5° tilt from both -65 to -50° and +50 to +65°. Such images clearly show the bicontinuous nature of the block copolymer microstructure. This material is available free of charge via the Internet at <http://pubs.acs.org>.

LA700507J

(30) Porte, G.; Appell, J.; Bassereau, P.; Marignan, J. *Journal De Physique* **1989**, *50*, 1335–1347.

(31) Sides, S. W.; Kim, B. J.; Kramer, E. J.; Fredrickson, G. H. *Phys. Rev. Lett.* **2006**, *96*, Art. No. 250601.

(32) Thompson, R. B.; Ginzburg, V. V.; Matsen, M. W.; Balazs, A. C. *Science* **2001**, *292*, 2469–2472.